

## DEVELOPMENT OF A METHOD TO TEST BAMBOO CULMS IN DIRECT TORSION

Daniel Chacón Revelo, University of Puerto Rico, Mayagüez, daniel.chacon@upr.edu  
Christopher Papadopoulos, University of Puerto Rico, Mayagüez, christopher.papadopoulos@upr.edu  
Felipe Acosta Costa, University of Puerto Rico, Mayagüez, felipe.acosta1@upr.edu  
Kent A. Harries, University of Pittsburgh, USA, kharries@pitt.edu  
Ali Saffar, University of Puerto Rico, Mayagüez, ali.saffar@upr.edu

### ABSTRACT

The development of a method for testing whole bamboo culms under direct torsion is described. The overall approach is an adaptation of the direct test for timber as describe in the ASTM D198-15 standard, which implements a universal testing machine to convert applied load into torque over a specimen. To realize such a torsion test requires developing a gripping fixture to induce torsion over bamboo specimens, which is a challenge, due to the naturally round nature of the bamboo culm. Several approaches are considered, including the use of cement/epoxy, wrapped cables, or bolted connections. An evaluation of each methodology was proposed to assess criteria such as slippage, failure mechanism, feasibility, assembly stability, repeatability, and safety. This study concludes that the use of non-shrink cement, to bond the culm to an exterior steel sleeve, is preferable, and provided an overall description of the testing regime proposed

### KEYWORDS

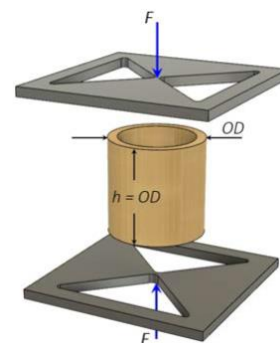
Bamboo; direct torsion; shear strength; ASTM D198-15.

### INTRODUCTION

It is well accepted that one key for adoption and acceptance of bamboo is to have standard procedures for mechanical testing, so as to lead to reliable understanding of its mechanical behavior and quality control. The current ISO 22157:2019 standard (ISO, 2019) prescribes methods for testing bamboo in bending (both parallel and perpendicular to the fibers), tension, compression, and shear. The shear test uses the “bow tie” method in which compression plates in which alternate quarters are offset or cut out, so that the corresponding alternate quarters of the culm can be “cut” or “slid” past each other. Figure 1 illustrates the plates used in the laboratory at the University of Puerto Rico, Mayagüez, and the schematic of how a cylindrical segment of the culm is tested.



(a)



(b)

**Figure 1.** Bow-tie shear plates (a) and illustration of how the cylindrical culm specimen is tested (b).

Another approach to obtaining shear strength for bamboo is to test the culm in direct torsion. This approach has not been widely attempted, and has not been standardized, but isolated attempts exist in the literature (Askarinejad, Kotowski, Shalchy, & Rahbar, 2015; Torres, 2005). A driving reason to investigate direct torsion of bamboo is to provide a directly comparable test as to what currently exists for conventional timber beams (ASTM International, 2015). The successful development of such a test would arguably elevate the credibility of bamboo as an alternative to timber. From a scientific point of view, comparison of result from the bow-tie shear test with the direct torsion test would be valuable, either to provide new insights into bamboo behavior if such results would be divergent, or to affirm the validity of the bow-tie test as a proxy for direct torsion in the case in which the results are convergent.

This article provides a discussion of the methodology being developed for the direct torsion test at University of Puerto Rico, Mayagüez, which is the subject of the Master's thesis of the author Daniel Chacón. As will be seen, the methodology is an adaptation of the method used for timber in the ASTM D198, but with dedicated approaches anchoring the nearly round bamboo culm into the loading elements of the testing apparatus.

### OVERALL STRATEGY

Following the concept provided in the D198 standard, the overall strategy adopted is to fix the bamboo culm between two “lever arms”, which directly apply the torque. The lever arms are loaded anti-symmetrically by a “loading beam”, which is driven by a load head from a mechanical testing machine. The overall scheme is illustrated in Figure 2. Of note is that as the crosshead moves down, the specimen also moves down. A discussion of how to attach the bamboo specimen to the loading arms is provided in the next section.

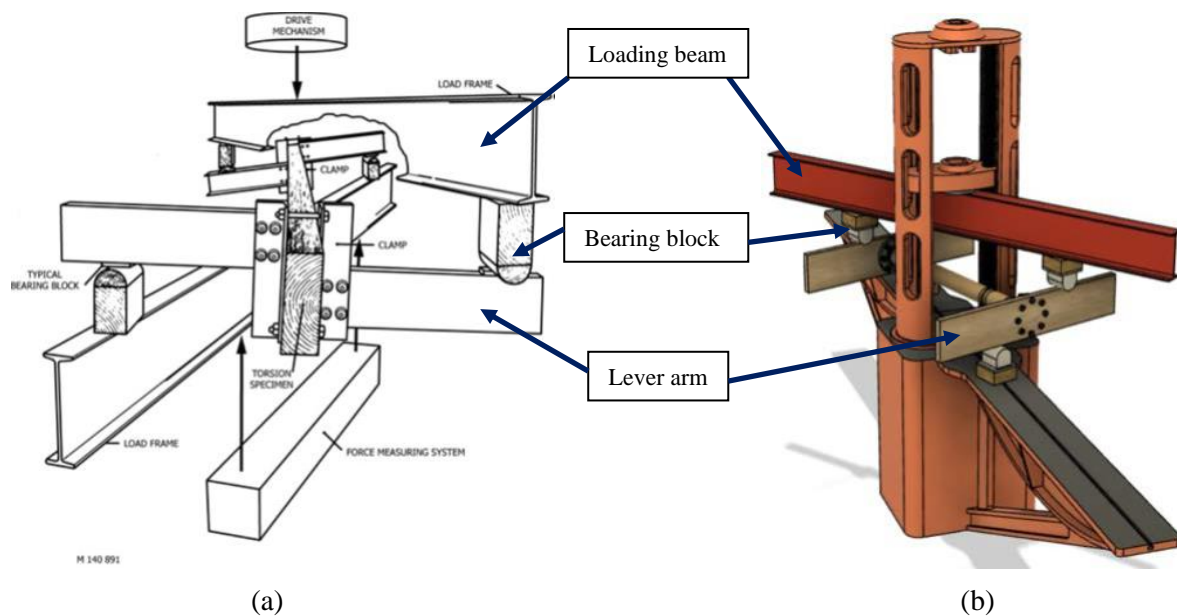


**Figure 2.** (a) The schematic for the test configuration as provided in ASTM D198-15. (b) Rendition of the first conceptualization for the bamboo test. In each figure, the “loading beam” is the I-beam that transmits the load from the load head to the “lever arms”, which are the parts of the apparatus that directly apply the torque to the specimen.

The design of this test is intuitive and has the advantage that uses a standard testing machine, which is likely to be present in a basic mechanical testing laboratory. Further, the testing machine, with this

configuration, is capable to apply the required loads. The bamboo species tested at UPRM is the locally available *Bambusa vulgaris*, which typically has a diameter of 3-3.5 in (75-90 mm) and wall thickness of 0.2-0.3 in (5-8 mm). Using a nominal shear strength of 3 ksi (21 MPa), an applied torque of at least 20 kip-in (2.25 kNm) is required. Even larger torques would be required to test larger sections that might occur in other locations. Acquiring a direct torsion machine with such a capacity would be costly.

A comparison of Figures 2a and 2b reveals a subtlety that was only recently appreciated by the authors. In Figure 2a, the lever arm is a composite body constructed such that both the applied load and the bearing block contact the lever arm along the *same central line* of the lever arm. In contrast, in Figure 2b, the lever arm consists of a single board of timber such that the applied load is transmitted to the top edge, and the bearing block reacts on the bottom edge; that is, the applied load and corresponding reaction occur on different parallel lines, separated by the depth of the lever arm.

Initially, the configuration in Figure 2b was chosen due to its simplicity. However, with this setup, during the test, the loading beam rotates about the vertical axis such that it runs into the tower of the testing machine. The authors have recently reflected on this and now believe that modifying the loading arm to a form similar to what appears in Figure 2a will both eliminate this rotation and provide a more accurate calculation for the calculated torque (see Figure 8b). The development of a precise rationale for this conclusion is currently in progress. The authors have found no discussion of this issue in the D198 standard or in related articles in which the D198 standard was applied for direct torsion of timber (Yang, Clouston, & Schreyer, 2013).

### ANCHORING BAMBOO TO THE LEVER ARMS

A fundamental challenge in developing a direct torsion test for bamboo is to fix the bamboo to the lever arm in a manner that eliminates or nearly eliminates rotational slipping of the culm relative to the fixture. As seen in Figure 2a, the design of the lever arm configuration takes advantage of the inherently rectangular form of the timber cross section, through which torque can be transmitted principally via normal contact. In contrast, bamboo is nearly round, and a fundamentally different strategy is necessary, either by normal contact from elements that might penetrate the cross section, or by frictional contact around the outer surface. Figure 3 shows several concepts for gripping bamboo.

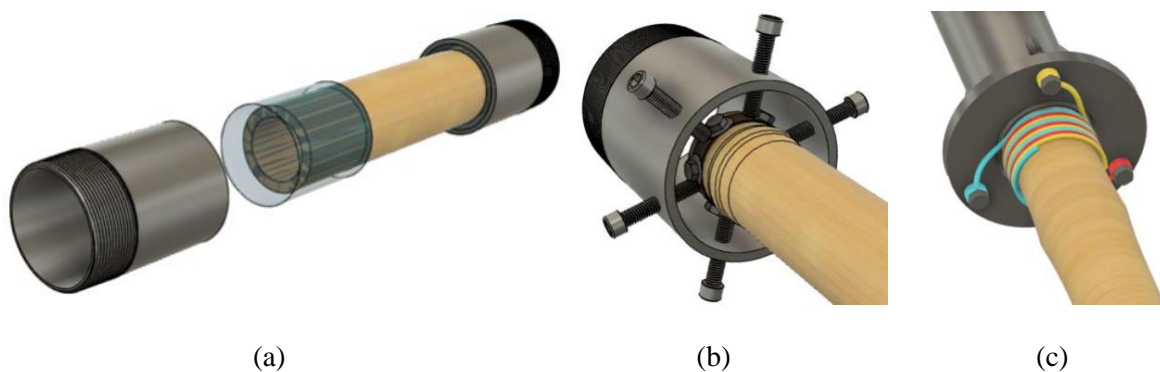


**Figure 3.** Approaches to transmit torque to the bamboo culm specimen: (a) Fixing the end of the culm to an outer sleeve, using cement or epoxy; (b) The “bolted sleeve”, which transmits torque by bolts attached to the sleeve to bolt heads of bolts that pass through the culm wall; (c) Wire gripping, using a cable or rope, in which the “belt friction” accumulates exponentially with increased wrapping.

Of the options considered, the authors have focused on the approach illustrated in Figure 3a, primarily due to its simplicity and practicality. Based on the nominal diameter of the specimens, a section of a Schedule 40 steel pipe with inside diameter 4 in (100 mm) is selected to surround the end of the culm, with the gap filled with a non-shrink cement (the wall thickness was tapered with a lathe to allow for a gradual reduction in stiffness from the flange to the specimen). This method relies on friction at the interfaces (steel-cement and cement-steel) to transmit torque, with a traction of 1 ksi (7 MPa) assumed

in determining the required length of the contact zone (2-3 in, or 50-75 mm). The steel pipe has the further advantage that the ends can be threaded, allowing a connection to a flange, which can then easily be bolted to the lever arm. The flange also allows for threaded rods to be used to help align and fix the specimen as the cement is placed. Finally, at the conclusion of the test, the cement anchor can be pushed out using a steel cylinder and the testing machine, allowing for unlimited reuse of the sleeves<sup>1</sup>. Figure 4 illustrates how the culm is cemented and then attached to the lever arms.

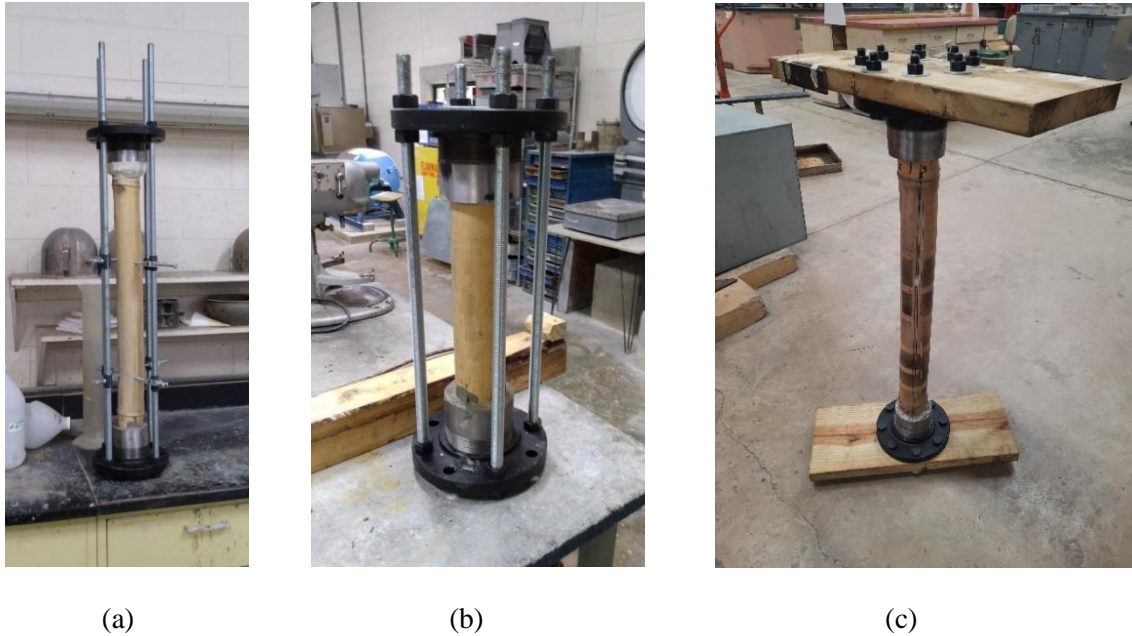


**Figure 4.** (a-b) To mount and align the bamboo, the flanges are first aligned using threaded rods. Then the culm can be inserted such that it is centered at each sleeve, with the aid of guide screws (a) when necessary. Figure (a) illustrates a long specimen with internodes, approximately 30 in (750 mm) in length, and Figure (b) illustrates a short specimen without nodes, approximately 18 in (450 mm) in length. (c) After the cement is sufficiently cured, the flanges are then bolted to the lever arms, which may or may not be chosen to be initially parallel, possibly to allow a greater range of motion during the test.

The approach in Figure 3b is similar to that used by (Askarinejad et al., 2015). Here, holes are drilled through the culm wall at 60° intervals, with short “inner” bolts inserted and tightened with nuts. Then, longer “outer” bolts that pass through the sleeve would bear on the inner bolt heads, driving the culm in a torsional manner via normal contact of the inner bolt bearing on the surface of the hole in the wall; additional frictional contact might be possible by inserting a rough sand paper between the inner bolt heads and the culm surface (this is illustrated by the dark band in Figure 3b). This method was not yet attempted on the basis that each specimen would require precision drilling to ensure approximately equal distribution of the load transfer, and also because this type of end condition would introduce artificial effects that could distort the apparent effects of applied torque. First, the effect of the hole and/or bolt bearing in the hold could lead to premature splitting, although the authors of (Askarinejad et al., 2015) indicate that this did not occur in their tests. Second, the presence of the bolts could add a constraint to impede longitudinal deformation as the culm deforms, and ultimately fails (this will be discussed in the next section on Failure).

The wrapping of a cable or rope around the culm, as shown in Figure 3c, is intriguing, and was initially attempted. The theory of belt friction implies that with enough wrapping, a sufficiently large tension can be developed in the cable or rope, and this concept was demonstrated in a preliminary test.

---

<sup>1</sup> Epoxy can be considered as an alternative to cement, but it is more difficult to cleanly remove from the sleeves after the test.



However, the practicalities of this approach have not yet been mastered. First, in the case of steel wire rope (1/8 in or 3 mm), the wire rope has enough bending stiffness that it needs to be pre-wound around a small cylinder so that it will have a permanently smaller radius of curvature in the zero-tension state. The possibility of a sudden rupture or pull out of a wire rope could also lead to a safety issue. The stiffness also makes attachment to the lever arm difficult. An alternative is to use a nylon rope, which has negligible bending stiffness, but it is difficult to control slipping against of the rope against the culm, it is difficult to account for the stretching of the cable in the apparatus, and it is also tedious to attach the rope to the lever arm. Nevertheless, the shape-conforming nature of the nylon rope, along with the apparent fact that the rope would impose negligible restraint in the longitudinal direction, lead the authors to believe that this approach is worth revisiting in the future. Figure 5 illustrates some of the initial attempts to mount the culm using wire rope or nylon rope.

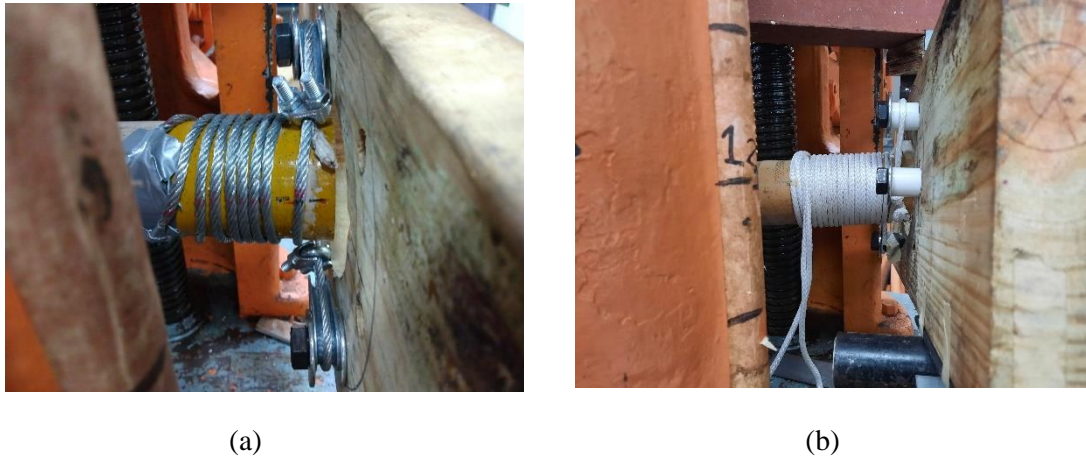


**Figure 5.** (a) Use of wire rope to mount the culm. (b) Use of nylon rope to mount the culm. Both cases present practical difficulties in mounting. Here, the ropes were attempted to be attached directly to bolts through the lever arm, without the flange.

## PRELIMINARY RESULTS

To date, the team has conducted several qualitative tests to understand the behavior of the apparatus and to make refinements. As was noted previously, the lever arm depicted in Figure 2b is currently being revised, but nevertheless, some other lessons have been learned using this initial design.

### Slipping

First, the preliminary results identified the types of inter-surface slipping that can occur. These are illustrated in Figure 6.

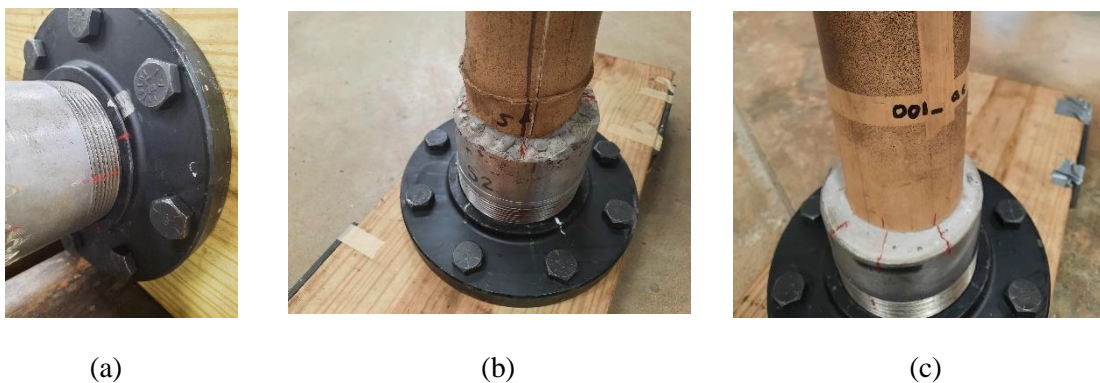


**Figure 6.** Slipping between (a) flange and sleeve, (b) sleeve and cement, and (c) cement and culm. Slippage is observed through the separation of the red lines that were initially marked before the test.

The major source of slipping occurred between the flange and sleeve, as indicated in Figure 6a. This was expected initially, but it was anticipated that eventually the sleeve would ‘lock’ into the flange. This problem has since been eliminated by welding the sleeve to the flange. A minor degree of slipping occurs between the sleeve and flange (Figure 6b). This is due to the essentially round character of the manufactured steel pipe. This effect can possibly be reduced by slightly deforming the sleeve to be ovalar. The slipping between the cement and culm is also relatively minor. This effect is mitigated by the slightly out-of-round character of the culm. It is also believed that as the cement is initially moist, the culm slightly swells, and the contracts as the system returns to ambient humidity. Therefore, testing within a few days of pouring, and/or curing in a plastic bag, could also mitigate this effect.

### Failure

Failure appears as a longitudinal crack parallel to the fiber orientation (more precisely, failure occurs along a plane whose normal is the circumferential direction, as defined from the zero stress reference configuration). This behavior is expected and is similar that which occurs in the “bow-tie” test. As the culm fails, the adjacent surfaces across the crack slip relative to one another, such that near the crack surface, the ends of the culm will display axial displacement, consistent with the shear overall shear deformation. This axial displacement is expressed as a protrusion of portions of the culm through the end of the cement anchor. Figure 7 illustrates this type of failure.

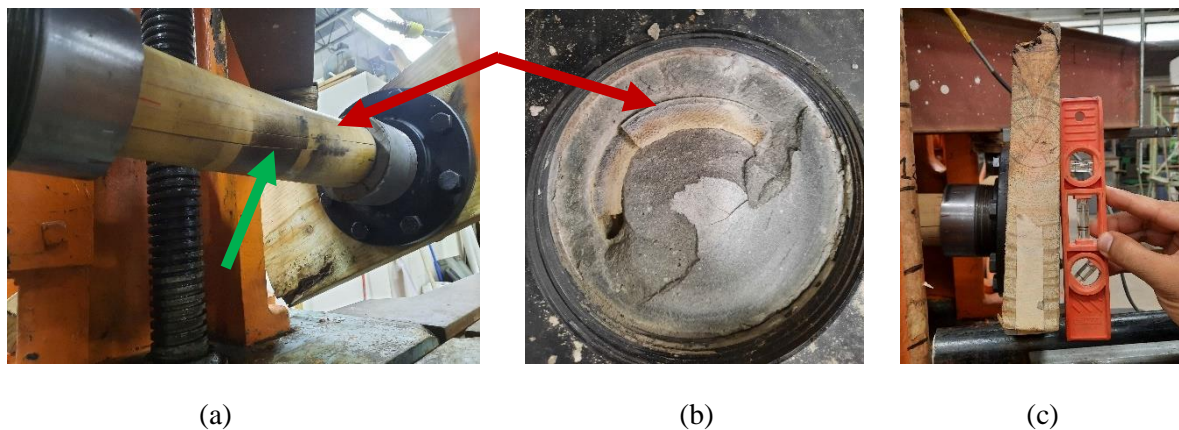


**Figure 7.** (a) The green arrow points to the failure plane, which appears as a longitudinal crack. The other longitudinal lines that appear were pre-existing hairline cracks. (b) The red arrows point to a section of the culm that protrudes through the end of the cement anchor. (c) The protruding segment of the culm causes a visible rotation of the lever arm about its central longitudinal axis.

The presence of the protrusion indicates the difficulty in developing an end condition that allows for pure torsion/shear, without the presence of other effects. Clearly, the cement provides a modicum of resistance against the natural tendency for the shear displacement, but the authors believe that this effect is less than what would occur in the bolted sleeve configuration. Perhaps the cable/rope approach would provide the closest approximation to a “pure” torque end condition, but as was noted before, the practicalities of implementing this setup have not yet been worked out.

### OTHER ASPECTS OF THE TEST UNDER DEVELOPMENT

Beyond the immediate physical aspects of the test setup, several other issues are in progress to enable accurate and repeatable measurements. Many of these issues relate to the geometry of the lever arm, which changes as the test is in progress. This is illustrated in Figure 8, below.

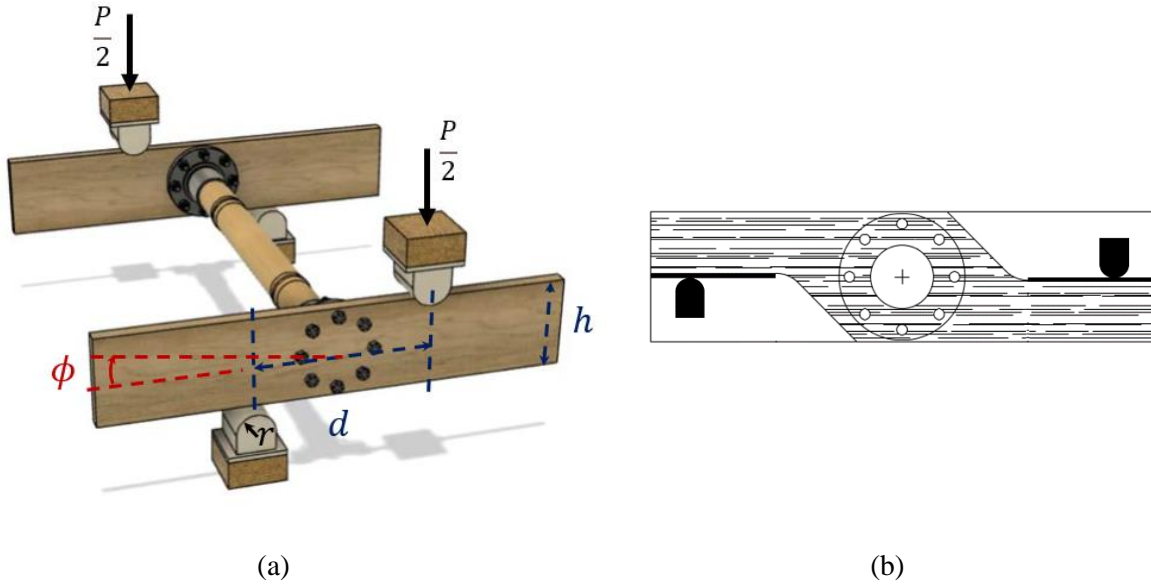


**Figure 8.** (a) Initial geometry of the lever arm:  $h$  represents the depth of the lever arm,  $d$  represents the initial separation distance between the bearing blocks,  $r$  represents the radius of the end of the bearing block, and  $\phi$  represents the angle of rotation of the lever arm about the central axis (aligned along the culm). (b) A rendition of the updated design of the lever arm such that effectively,  $h = 0$ .

The following issues are currently under development:

1. A load cell is used to measure the force  $P$  applied to the center of the loading beam, from which the applied torque can be estimated. Nominally, the applied torque is

$$T = \frac{P}{2}d \quad \text{Eq. 1}$$

where  $P$  is the applied load,  $d$  is the distance between the bearing block on the lever arm, and  $T$  is the applied torque. However, as the test is in progress, the lever arms will rotate (corresponding primarily to the twist of the culm, but to some degree, also accounting for rotational slippage). This means that the formula needs to be adjusted to account for the geometrical state. Under the assumption that the bearing blocks travel only vertically, the authors have derived the following formula for the applied torque,

$$T = \frac{P}{2\cos\phi(\cos\phi + \mu\sin\phi)} [d - (2r + h)\sin\phi + \mu h]. \quad \text{Eq. 2}$$

In Eq. 2 the interpretation of  $d$  is the *initial* separation distance at the beginning of the test; the bracketed term represents the fact that as the test progresses, the bearing blocks will slide relative to the lever arm, thus changing the actual distance of separation. Direct comparison of Eq. 2 with Eq. 1 indicates that many factors perturb the nominal estimation away from the nominal estimate in Eq. 1. These are primarily geometric in nature, but the coefficient of kinetic friction is also present. Considering that a protective steel bar is placed between the lever arm and the bearing block, the coefficient for steel-on-steel is approximately 0.35–0.50. A detailed estimate of this kind does not appear in the ASTM D198 standard, and another published estimate ignores the effect of friction (Yang et al., 2013).

Due to the lack of certainty of the coefficient of friction, the formula is at best a good estimate. For example, for typical dimensions  $d = 16$  in,  $r = 1.5$  in, and  $h = 0$ , at  $\phi = 0.50$  rad, which is plausible, the calculated value of  $T$  from Eq. 2 is 86% of the nominal value (Eq. 1) for  $\mu = 0.35$  and 80% of the nominal value for  $\mu = 0.50$ . Therefore, a second approach is in progress, which is to build a load cell using a steel tube with strain gauges, which would be installed between the lever arm and the specimen.

2. Direct measurement of strain in the specimen is not planned. The use of strain gauges is straightforward, but tedious. Use of digital image correlation is not straightforward in this situation, because a given speckled patch would both move vertically with the specimen and rotate, thus making it a 3D problem that requires a sophisticated camera system and software as well.
3. Direct measurement of both the rotation of the lever arm and twist of the specimen are planned. Because these are macroscopic quantities, they can be accurately measured by mounting cell phones with inclinometer apps. Similarly, cell phones can be mounted on the lever arms. Relative twist between the end points can then be calculated, from which the modulus of rigidity in the axial-circumferential plane can be estimated from the well-known formula

$$G = \frac{TL}{J\theta} \quad \text{Eq. 3}$$

where  $T$  is the applied torque,  $L$  is the length between the rotation measurement points,  $J$  is the polar moment of inertia of the cross section, and  $\theta$  is the measured relative angle of twist over the measurement segment. This will be an estimate because of the uncertainty in  $T$  as well as the fact that the culm is not perfectly round, so the formula does not exactly apply. However, as  $G$  is not estimated as part of the bow-tie shear test, this is a useful result.

4. Once the testing protocol is refined, batch tests will be taken on at least 20 culms and comparisons will be made to bow-tie shear tests on cylinders from neighboring nodal segments. It is nominally expected that the measured shear strength from the direct torsion test will be slightly higher than for the bow-tie test because the anchoring cement in the direct test adds a constraint that is not present in the bow-tie test.
5. Moisture content will be measured for all test specimens after testing. Given the humid environment of the laboratory, it is expected that the moisture content will be approximately 15%.

## CONCLUSIONS AND FUTURE WORK

A careful process is being undertaken at the University of Puerto Rico, Mayagüez to develop a direct torsion test for bamboo culms. Preliminary tests have informed some refinements, such as the redesign of the form of the lever arms, and the minimization of rotation between the sleeve and flange. The next phase of the research will involve calibrating the measured applied load to be interpreted as applied torque on the test culm. After this has been accomplished, a testing plan will be undertaken to compare shear strength calculated from the direct torsion test with that calculated from the bow-tie test with companion cylinders.

The development of this test will lead to a new standard for testing bamboo culms under direct torsion, allowing direct comparisons to be made with torsion of timber beams. However, in comparison to the bow-tie test, the direct torsion test is more complicated to conduct. Therefore, another possible outcome of this initiative will be to further validate the bow-tie shear test as a proxy for a direct torsion test.



## ACKNOWLEDGEMENT

This material is based upon work supported by the National Science Foundation under Grant Nos. 1634828 and 1634739.

## CONFLICT OF INTEREST

The authors declare that they have no conflicts of interest associated with the work presented in this paper.

## DATA AVAILABILITY

Data on which this paper is based is available from the authors upon reasonable request.

## BIBLIOGRAPHY

- Askarinejad, S., Kotowski, P., Shalchy, F., & Rahbar, N. (2015). Effects of humidity on shear behavior of bamboo. *Theoretical and Applied Mechanics Letters*, 5(6), 236–243. <https://doi.org/10.1016/j.taml.2015.11.007>
- ASTM International. (2015). *Standard Test Methods of Static Tests of Lumber in Structural Sizes* (Vol. ASTM D198-). <https://doi.org/10.1520/D0198-15>. Copyright
- ISO. (2019). *ISO 22157: Bamboo structures - Determination of physical and mechanical properties of bamboo culms - Test methods* (1st ed.). Geneva, Switzerland: International Organization for Standardization. Retrieved from <https://www.iso.org/standard/65950.html>
- Torres, L. (2005). *Modelo anisótropo de elementos finitos para el análisis mecánico del bambú y su verificación experimental*. Universidad del Valle, Colombia.
- Yang, Z., Clouston, P. L., & Schreyer, A. C. (2013). Torsional Shear Tests on Laminated Veneer Lumber Using a Universal-Type Test Torsional Shear Tests on Laminated Veneer Lumber Using a Universal-Type Test Machine. *Journal of Materials in Civil Engineering*, December, 1979–1983. [https://doi.org/10.1061/\(ASCE\)MT.1943-5533.0000752](https://doi.org/10.1061/(ASCE)MT.1943-5533.0000752)